Energy and Buildings 43 (2011) 1913–1918

Contents lists available at ScienceDirect

Energy and Buildings

journal homepage: www.elsevier.com/locate/enbuild

Studying the features of air flow induced by a room ceiling-fan

Ramadan Bassiouny*, Nader S. Korah

Department of Mech. Power Eng. & Energy, Minia University, Minia 61111, Egypt

ARTICLE INFO

Article history:
Received 8 June 2010
Received in revised form
18 December 2010
Accepted 26 March 2011

Keywords:
Ceiling fan
Air distribution
Ventilation

ABSTRACT

Creating a breeze in a space is necessary to enhance convective heat transfer and accordingly body heat dissipation. In most tropical countries, ceiling fans are extensively used to create an indoor breeze, improve the space air distribution and, hence enhance the feeling of comfort. The fan speed, diameter, number of blades, blade angle, and location all play an important role in determining the induced flow pattern features in the space.

Few previous studies have investigated fan induced flow and its characteristics under different geometric and operating conditions. In this study, an analytical as well as a computational model was used to predict the flow pattern induced by a ceiling fan into a selected space. The numerical and mathematical results were compared to published experimental data. The results showed that the flow pattern has different features as it leaves the fan and proceeds towards the floor. It has a divergence angle of almost 150°. Two correlations are introduced to help predicting the air velocity distribution due to using a ceiling fan.

1. Introduction

People feel discomfort when they get sweat in a space with a stagnant air. Therefore, people try to create air breeze around their bodies either naturally or mechanically to enhance body convective heat transfer. Air motion helps sweat evaporation and, accordingly brings body comfort feeling.

It is very difficult for many people in developing countries to have an air conditioner to achieve indoor comfort conditions. Instead, people depend mainly on natural ventilation; if aeromotive forces due to the wind, or stack effect exist. Ceiling fans are used in offices, residences as an alternative to extend the summer comfort envelope. These fans are of affordable cost, simple in construction, easy to install, and do not need regular or sophisticated maintenance.

The flow-pattern features induced by ceiling fans are very helpful for people of interest working in the field of HVAC. This flow is expected to be rotational, three-dimensional and turbulent. So, knowing the flow characteristics, as a result of ceiling-fan rotation would help improving the fan design in addition to selecting its optimum placement to save energy. Further in air conditioned spaces, turning a ceiling fan on would help reaching the space controlled uniform temperature much faster than if there is no ceiling fan.

Ankur et al. [1] experimentally investigated the flow field of a ceiling fan in a full-scale space with no furniture. In this study, they identified different flow regions in the space through smoke visualization. In the same study they compared the effect of using winglets or spikes at the blade tip on improving the induced flow pattern and breaking down the tip vortices.

The authors [1] performed their experimental study on a full-scale room of 3.6 m × 3.6 m with a height of 3.0 m using a 1200 mm-diameter fan with a maximum speed of 240 rpm. They identified the flow pattern into different regions. A cylindrical cone region with a 10° cone angle with the fan vertical axis extending downward below the fan is characterized by the highest velocities in the room, and covers a large portion of the floor area. Another thin region is adjacent to the room walls with an upward velocity; then, a region sandwiched between the previous two regions exists and is characterized by small velocities (less than 0.1 m/s). Finally, a region of vortices is seen at the blade tip, and a region of flow entering the fan plane from above. In the same study, they presented a quantitative variation of air velocity in the room at two planes of two different heights measured from the floor.

Schmidt and Patterson [2] studied the performance of a new high efficiency design of a ceiling fan with aerodynamic blades versus conventional fans. They concluded that the new ceiling-fan design can decrease the power consumption by a factor up to three, compared to the conventional ceiling fans.

Rohles et al. [3] studied the effect of using a ceiling fan running below a false, high-ceiling in an open zone, at different heights above the floor. They found that the velocities were the same with or without the ceiling existence. They recommended the proper

* Corresponding author. Tel.: +20 16 391 6415; fax: +20 86 2346674.
E-mail address: ramadan9@yahoo.com (R. Bassiouny).

0378-7788/$ – see front matter © 2011 Elsevier B.V. All rights reserved.
doi:10.1016/j.enbuild.2011.03.034

Nomenclature

D	space depth (m)
H	height (m)
P	pressure (N m^{-2})
R	fan radius (m)
u, v	velocity components (m s^{-1})
W	space width (m)
$x_{i,j}$	space coordinate system, i, j = 1,2

Subscripts

f	fan
r	radial, used for fan axis in fan-plane
w	wall
θ	tangential, used for fan axis in fan-plane
z	downward direction

Greek letters

ρ	air density (kg m^{-3})
μ	dynamic viscosity (kg m^{-1} s^{-1})
ν	kinematic viscosity (m^2 s^{-1})
τ	wall shear stress (N m^{-2})
δ	boundary layer thickness (mm)

placement of measurements and the enough number of measurement points (10 points) per location. They added that air velocities diminished very rapidly beyond almost 40% of the height from the fan hub.

Rohles et al., in another study, [4] reported that ceiling fan manufactures claim that air of 28 °C with a running ceiling fan will provide the same amount of comfort as 24 °C without a fan. They added that the turbulence and variable-characteristics of the air plume, due to the ceiling fan, may be its major comfort-producing feature. In the same article, the authors mentioned that ASHRAE stated in their standards that loose paper, hair, and other light objects may start to be blown about at an air velocity of 0.8 m/s.

Thorshauge [5] studied the velocity fluctuations in 12 different-volume ventilated spaces. The author mentioned that the velocity fluctuations were not periodic but intermittent. A linear relationship between the mean velocity and standard deviation, maximum velocity, mean acceleration, and standard deviation of the acceleration was found. Neither the space volume, supply flow, nor the type of outlet had any significant influence on this linear relationship.

Son et al. [6] studied the effect of using a ceiling fan along with an air conditioner on human thermal comfort. They found that without the use or with a little use of the ceiling fan, thermal comfort is strongly dependent on the location of the inlet diffuser. However, thermal comfort has a strong dependence on the vertical air speed due to the fan.

Schiavon and Melikov [7] investigated the effect of elevating air speed in a space on potential saving of cooling energy. They reported that the required power input of the supplied fan is a critical factor that achieves energy saving at elevated room temperature. However, they added that under their assumptions, energy saving may not be achieved with ceiling, standing, tower and desk fans widely used when the power consumption of the fan is higher than 20 W.

2. Mathematical analysis

Flow induced by a ceiling fan is mainly 3D and rotational, particularly in the fan plane. This rotation effect starts to decrease once the flow is forced downward into the space. Below is a mathematical formulation that can help predicting both the radial distribution of the tangential velocity in the fan plane as well as the downward velocity. The governing momentum equations in the tensor form can be written as (Tannehill et al. [8]):

$$\rho\left(u_j\frac{\partial u_i}{\partial x_j}\right) = -\frac{\partial p_i}{\partial x_i} + \mu\left[\frac{\partial}{\partial x_j}\left(\frac{\partial u_i}{\partial x_j} + \frac{\partial u_j}{\partial x_i}\right)\right] \tag{1}$$

Since the present study focuses on flow pattern in two different planes in the space: the fan plane, and a mid-space downward plane, two different coordinate systems are considered. It is expected that the flow is rotational in the fan plane; therefore, the cylindrical coordinate system is considered; while the Cartesian coordinate system is used with the mid-space downward plane.

When analyzing flow in the fan plane, the following assumptions are adopted to simplify the model:

- The flow is mainly rotational, i.e. $v_\theta \gg v_r$.
- The fan rotational-speed is uniform, and the blades are identical, i.e. $v_\theta(r)$ is only considered.
- The angular pressure gradient, $\partial p/\partial\theta$, is neglected.

Applying these assumptions on the θ-momentum of Eq. (1) as shown below:

$$\rho\left(v_r\frac{\partial v_\theta}{\partial r} + \frac{v_\theta}{r}\frac{\partial v_\theta}{\partial\theta} + \frac{v_r v_\theta}{r}\right) = \frac{-1}{r}\frac{\partial p}{\partial\theta} + \mu\left(\frac{\partial}{\partial r}\left(\frac{1}{r}\frac{\partial}{\partial r}(rv_\theta)\right) + \frac{1}{r^2}\frac{\partial^2 v_\theta}{\partial\theta^2} + \frac{2}{r^2}\frac{\partial v_r}{\partial\theta}\right) \tag{2}$$

leads to the following partial differential equation in the polar form:

$$r^2\frac{d^2 v_\theta}{dr^2} + r\frac{dv_\theta}{dr} - v_\theta = 0 \tag{3}$$

This equation is in the form of Cauchy equation with a solution in the form of (Trim [9]):

$$v_\theta = C_1 r + \frac{C_2}{r} \tag{4}$$

The constants can be obtained from Dirichlet-type boundary conditions in the form:

$$v_\theta(R) = \omega R, \quad \text{and} \quad v_\theta\left(\frac{W}{2}\right) = 0$$

where ω is the fan angular velocity. Applying the two boundary conditions in the solution leads to the following distribution:

$$v_\theta(r) = \frac{\omega R^2}{1-(2R/W)^2}\left[\frac{1}{r} - \frac{4r}{W^2}\right] \quad R \le r < \frac{W}{2} \tag{5}$$

For the distribution of the downward velocity, a flow analysis in a mid-plane, as shown in Fig. 1, is carried out. Similar assumptions to that mentioned earlier are adopted to simplify the governing equations to be solved. Assuming that the downward velocity is dominant compared to the other components; hence, the governing momentum equation, considering the continuity equation, can be reduced to the Laplace equation:

$$\frac{\partial^2 v_z}{\partial x^2} + \frac{\partial^2 v_z}{\partial z^2} = 0 \tag{6}$$

The boundary conditions in this case are as follows; taking z measured from the floor and upward:

$$v_z(x, H_f) = f(x), \quad v_z(x, 0) = 0,$$

$$\frac{\partial v_z}{\partial x}(0, z) = 0, \quad \text{and} \quad v_z\left(\frac{W}{2}, z\right) = 0 \tag{7}$$

The method of separation of variables (Trim [9]) is employed to solve Eq. (6) along with the accompanied boundary conditions, Eq.

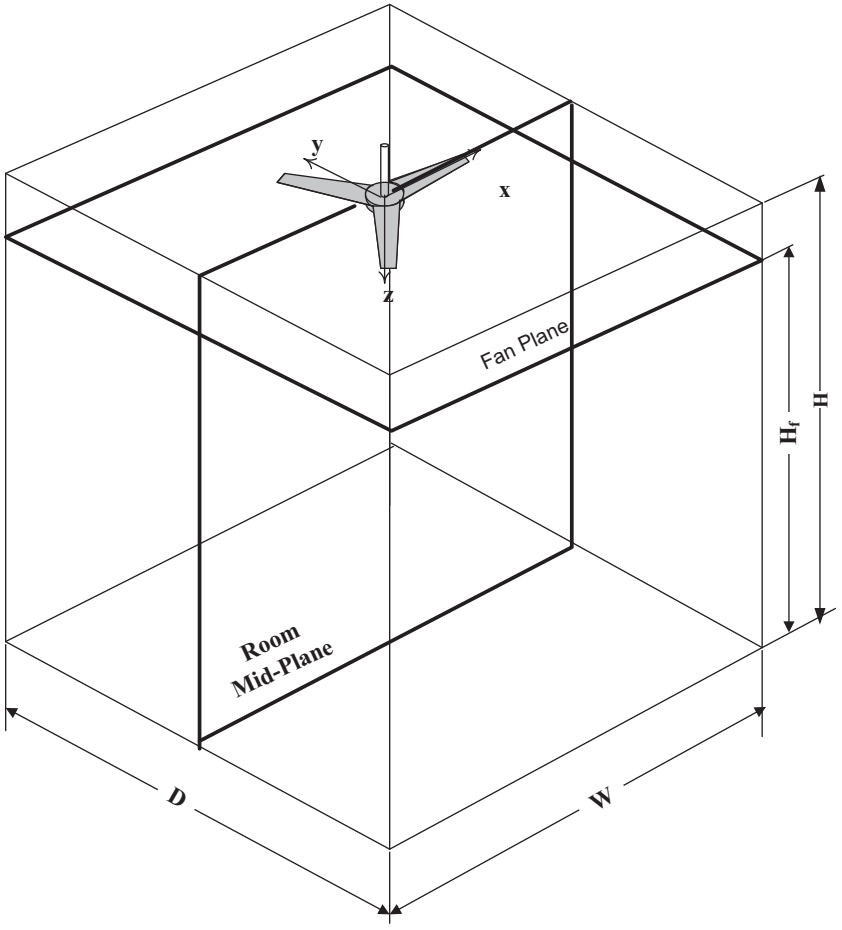

Fig. 1. A general layout of a room with a ceiling fan showing the planes of interest.

(7). The solution is in the following form:

$$v_z(x,z) = \sum_{n=1}^{\infty} C_n \cdot \sinh(\lambda z) \cdot \cos(\lambda x), \quad 0 \le z < H_f,$$

$$\text{and} \quad 0 \le x \le \frac{W}{2} \tag{8}$$

where $C_n = (4/(W \sinh \lambda H_f)) \int_0^{W/2} f(x) \cos \lambda x \, dx$, and $\lambda = ((2n-1)/W)\pi$.

It is worthy to mention that a fitting correlation, based on measured experimental results by Ankur et al. [1], was predicted in the form of:

$$v_z(x, H_f) = a_0 + a_1 x + a_2 x^2 + a_3 x^3 + a_4 x^4 + a_5 x^5$$

The coefficients of this polynomial are tabulated as follows:

a_0	a_1	a_2	a_3	a_4	a_5
1.6707	−8.2639	178.9714	−771.7363	1163.4398	−585.2967

The above correlation was fitted with an R-square of 98%. Both equations ((5) and (8)) can be used to predict the velocity distribution in the fan plane and downward of the fan till the space floor, within the restricted dimensions. However, the equations can be readjusted for different fan sizes and space dimensions.

3. Computational analysis

Experimental flow visualization to depict flow pattern due to ceiling fans is neither easy nor simple. The computational fluid dynamics has been extensively and promisingly used in many complicated applications. In the present study, a finite-element based commercial code, Ansys, is used to simulate the flow pattern induced by a ceiling fan in a space. It is very important to study this problem in the view of 3D including furniture in the space. However, our point of view here is to get benefit from the flow similarity extending below the fan and around its vertical axis, and to predict the flow pattern based on which a seating zone can be adopted. Therefore, two planes of importance were chosen: the fan plane, and a vertical mid-plane passing through the fan rotation axis. Fig. 1 shows the physical domain configuration with the two studied planes.

In order to count for the turbulence effect, the two-equation, k–ε, model is adopted to predict the turbulence viscosity based on the turbulence kinetic energy and its dissipation. In this model, the turbulent viscosity is related to the turbulence kinetic energy, k, and dissipation rate, ε by the Prandtl–Kolmogorov as follows:

$\mu_t = \frac{C_\mu \rho k^2}{\varepsilon}$, where $C_\mu = 0.09$.

Knowing an inlet velocity, the program calculates the turbulence kinetic energy and its dissipation at the inlet, based on an inlet intensity of turbulence and an inlet length scale factor. The program uses the following equations:

$$k_{\text{inlet}} = \frac{3}{2}[\text{inlet intensity} \times V_{\text{in}}]^2 \quad \text{and} \quad \varepsilon_{\text{inlet}} = \frac{C_\mu k^{3/2}}{\text{inlet scale factor} \times L_C}$$

where L_C is a characteristic length such as an inlet diameter, hydraulic diameter, or plate length. Directly below the fan, the diameter is taken as 90% of the tip diameter of the fan, as men-

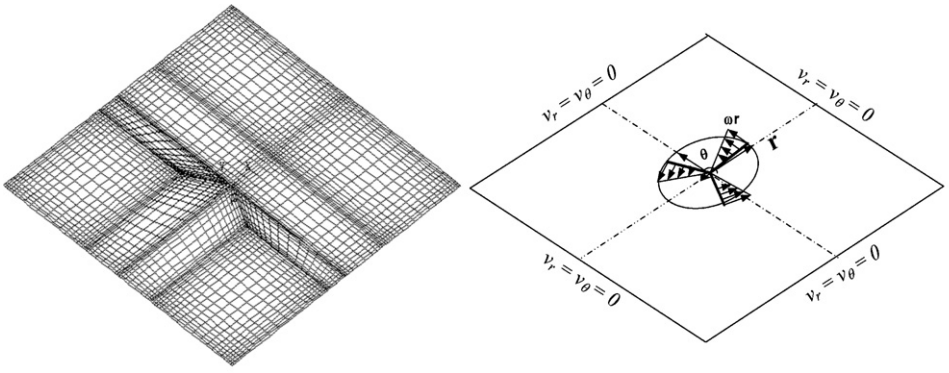

(a) Fan Plane: Grid configuration (left), Boundary conditions (right)

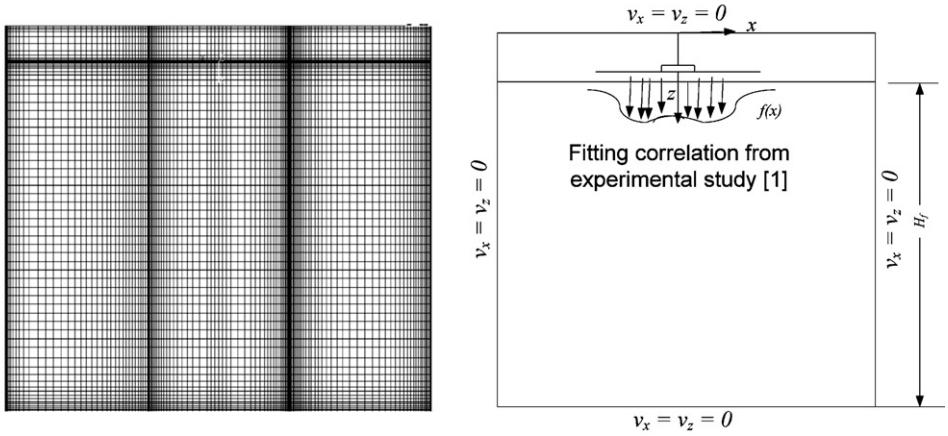

(b) Room Mid-Plane: Grid configuration (left), Boundary conditions (right)

Fig. 2. The computational domain of the selected planes.

tioned in [1]. The product term of inlet intensity and velocity gives the fluctuating velocity component at the inlet. The inlet intensity default is taken 0.01, corresponding to a level of turbulence of 1% at the inlet. The length scale at inlet region is a multiple of a characteristic length and an inlet scale factor taken as 0.01 in the present study.

The two-equation model assumes a fully developed turbulent flow, which is not the case in the sublayer region near the wall, where viscous effects are dominant. Therefore, a wall turbulence model called the log-law of the wall is a remedy along with the k–ε model. This law of the wall is given as (Tannehill et al. [8]):

$$U_w/\sqrt{\frac{\tau_w}{\rho_w}} = \frac{1}{\kappa}\left[\ell n \frac{E\delta}{\nu}\sqrt{\frac{\tau_w}{\rho_w}}\right]$$

The values of κ (the von Karman constant), and E (a roughness parameter) are 0.4 and 9.0, respectively.

The computational domains of both planes, shown in Fig. 1, are indicated in Fig. 2a and b, respectively. The boundary conditions are shown along with the computational domain for the fan plane as well as for the vertical plane. Since it is not easy to specify the inlet boundary conditions for the vertical plane, a Dirichlet-type of boundary conditions is taken from real measurements of Ankur et al. [1] for the downward velocity and then applied just below the fan to help predicting the velocity distribution downward the fan towards the floor.

A quadrilateral type-of-element with a quadratic approximation function was adopted. In the fan plane, the discretized momentum equations in the radial and tangential directions were iteratively solved for a steady state assumption.

In order to prove a grid-independent solution, a successive mesh refinement was adopted till the grid configuration for the fan plane was 2800 elements, and for the mid-plane was 8442 elements. Mesh refinement was applied in regions of expected sharp variation of the variables; such that the model can capture this variation. The semi-iterative tri-diagonal matrix algorithm, TDMA, is used to solve the assembled matrix of unknowns.

4. Results and discussion

Fig. 3a shows a qualitative enlarged portion of the velocity vectors around the fan rotating-blades. It can be seen the swirl behavior due to the fan rotation. As the fan rotates, the air layers attached to the blades randomly rotate. Due to air viscosity and molecules attraction forces, the rotation effect transfers to the air in the fan plane and progress downward. The dense zones in the figure are the places of maximum tangential velocities at the blade tip. But, this velocity decreases as air moves towards the space walls. Quantitatively, Fig. 3b illustrates the air velocity contours as a result of running a ceiling fan into the space. The figure presents the velocity variation from the fan centerline to the bounded walls. This figure supports the pattern shown in Fig. 3a, and reinforces the flow symmetry.

The tangential velocity variation at some distances from the fan blade is shown in Fig. 4. The figure indicates that increasing the fan speed by a factor of four would almost increase the tangential velocity by the same factor. The figure also illustrates that the air velocity decreases at some distance away from the fan blades. Fig. 4 shows a comparison between the numerically predicted results with the mathematically calculated ones based on Eq. (4). A reasonable trend

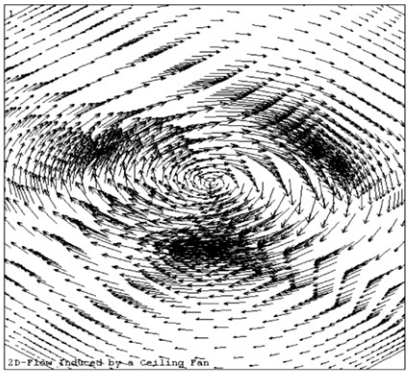

(a) Enlarged Portion of Velocity Vectors near the Fan Blades

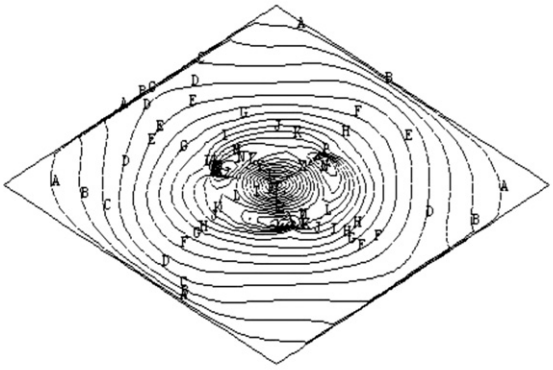

m/s
A =.41883
B =1.257
C =2.094
D =2.932
E =3.77
F =4.607
G =5.445
H =6.283
I =7.12
J =7.958
K =8.796
L =9.633
M =10.471
N =11.309
O =12.146
P =12.984
Q =13.822
R =14.659

(b) Velocity contours at the Fan Plane

Fig. 3. Flow pattern induced by the fan on its plane of rotation.

match was noticed for the four different rotational speeds. The computational results obtained by Ansys showed underprediction trends due to the carried assumptions to model the problem. The fan plane might be of a little interest for the HVAC people, who are usually interested in the occupied zone, which is almost 1.8 m above the floor. However, the information obtained in the fan plane might help the fan designers and people of interest to improve the fan design and configuration.

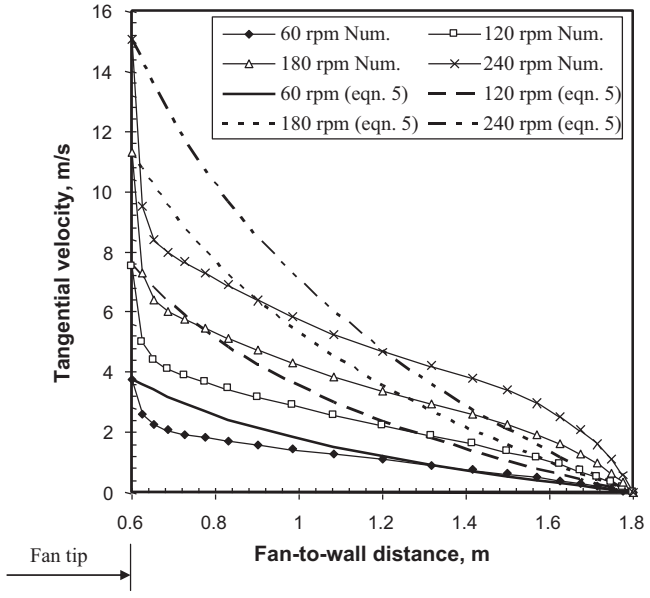

Fig. 4. Tangential velocity variation in the fan plane at different rotation speeds.

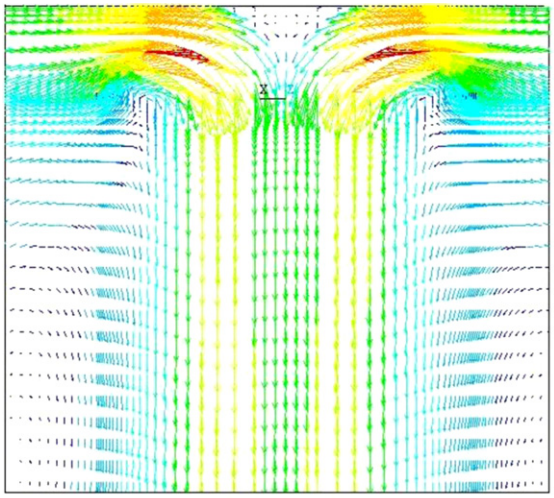

(a) Enlarged Portion of Velocity Vectors Directly below the Fan

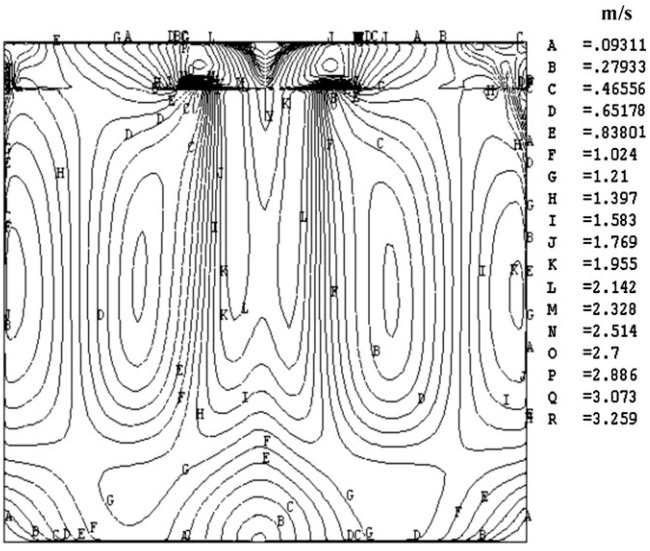

m/s
A =.09311
B =.27933
C =.46556
D =.65178
E =.83801
F =1.024
G =1.21
H =1.397
I =1.583
J =1.769
K =1.955
L =2.142
M =2.328
N =2.514
O =2.7
P =2.886
Q =3.073
R =3.259

(b) Velocity contours at the Room Mid-Plane

Fig. 5. Flow pattern induced by the fan on the room mid-plane below the fan.

The downward velocity variation is of great importance since it directly produces the velocity movement in the occupied zone. Fig. 5a indicates a qualitative enlarged portion of the flow behavior near the fan blades. The figure clearly illustrates the downward velocity progressively entering the occupied zone. The flow entrained by the fan towards its center of rotation can be seen above the fan plane. A velocity contour configuration for the whole domain is indicated in Fig. 5b. The figure shows a symmetric behavior about the fan axis and an air plume from the fan into the space. A velocity relax is observed as the air plume progresses towards the space floor.

Fig. 6 depicts a qualitative velocity distribution at different room planes from the fan plane to the floor. The purpose of this figure is to trace the flow behavior as it enters the occupied zone. It clearly shows the divergence zone below the fan forming a cone-like region. In addition, a reverse upward flow close to the walls is noticed due to the continuous entrainment of space air and its discharge downward. The effect of fan hub is clearly shown in the profile very near to the fan plane. This effect diminishes as flow proceeds towards the floor.

Available experimental results by Ankur et al. [1] were used to validate and judge the computational and analytical results. They

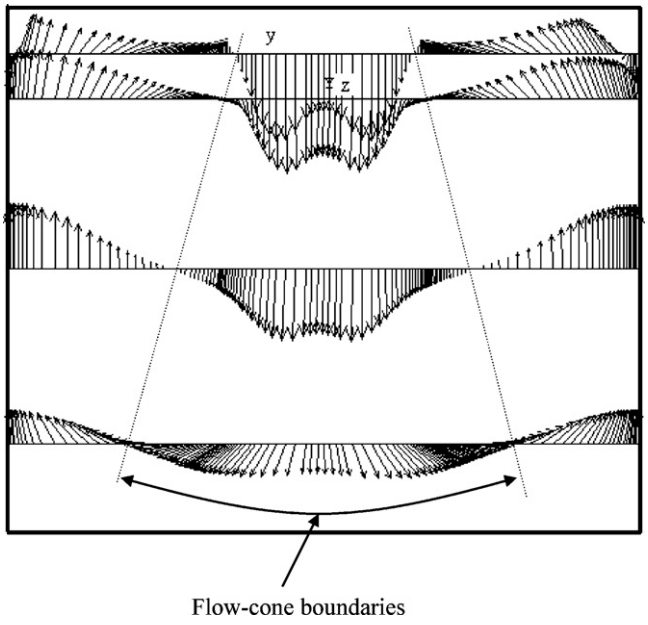

Fig. 6. A Qualitative depiction of flow pattern induced by the fan at selected planes below the fan-plane.

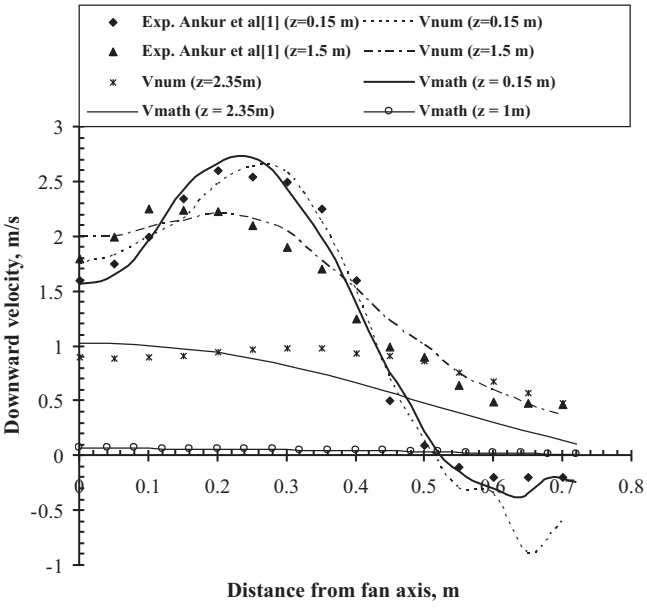

Fig. 7. Downward velocity variation at two planes below the fan compared with measured values by Ankur et al. [1].

showed quantitative velocity values in two planes parallel to the fan plane at distances 2.72 m and 1.5 m measured from the floor. Fig. 7 shows the downward velocity variation from the fan axis towards the room wall. A comparison between the measured values and the predicted ones at different planes are included in the figure. The figure illustrates a reasonable agreement in the velocity variation. The values corresponding to $z = 2.72$ m are the inlet values to the computational and mathematical models. It is seen from the figure that the air velocity is decaying as distance increases from the fan axis towards the wall. It is noticed that the fan outflow effect is gradually decreasing at a distance slightly greater than the fan diameter. As the air leaves the fan and proceeds towards the occupied zone, a velocity decrease is also noticed due to entraining room air form other parts and flow relaxation.

5. Conclusions

This study presented qualitative as well as quantitative figures of flow features induced by a ceiling fan. The results depicted different flow regions with specific characteristics inside the space. A downward flow zone with specific features was noticed. This may help adjusting the seating area, particularly in places where natural ventilation is not felt or not available.

The results showed that increasing the fan rotational speed results in increasing the local downward velocity distribution inside the space. Hence, operating a ceiling-fan at an improper rotational-speed may cause disturbance for occupants. Further, the study introduced two empirical correlations that can be used to predict the induced-air velocity distribution in a space from the fan plane downward towards the space floor with reasonable approximation values.

References

[1] J. Ankur, R.U. Rochan, C. Samarth, S. Manish, K. Sunil, Experimental investigation of the flow field of a ceiling fan, in: ASME Heat Transfer/Fluids Engineering Summer Conference, Charlotte, NC, USA, July 11–15, 2004.
[2] K. Schmidt, D.J. Patterson, Performance results for a high efficiency tropical ceiling fan and comparisons with conventional fans, Renewable Energy 22 (2001) 169–176.
[3] F.H. Rohles, S.A. Kons, B.W. Jones, Ceiling fans as extenders of the summer comfort envelope, ASHRAE Transactions 89 (part A1) (1983) 245–262.
[4] F.H. Rohles, J.E. Laviana, T.E. Shrimlin, Assessing air velocities from the industrial ceiling fan, ASHRAE Transactions 89 (part A1) (1983) 288–304.
[5] J. Thorshauge, Air-velocity fluctuations in the occupied zone of ventilated spaces, ASHRAE Transactions 88 (Part II) (1982) 753–764.
[6] Son H. Ho, Luis Rosario, Muhammad M. Rahman, Effect of using ceiling fan on human thermal comfort in air-conditioned space, in: AIAA 5734, 3rd Intl. Energy Conversion, 2005.
[7] Stefano Schiavon, Arsen K. Melikov, Energy saving and improved comfort by increased air movement, Energy and Buildings 40 (2008) 1954–1960.
[8] J.C. Tannehill, D.A. Anderson, R.H. Pletcher, Computational Fluid Mechanics and Heat Transfer, Taylor & Francis, USA, 1997.
[9] W. Trim Donald, Applied Partial Differential Equations, PWS-KENT Publishing Co., Boston, USA, 1990.